

Yielding transition under oscillatory shear in metallic glasses

Nannan Ren(任楠楠), Tiantian Meng(孟天天), Hui Huang(黄慧), Qunshuang Ma(马群双), Jun Fang(房军), Qin Li(李勤), and Weihuo Li(李维火)

Citation: Chin. Phys. B, 2026, 35 (**1**): 016103. DOI: 10.1088/1674-1056/ae2c6c
http://cpb.iphy.ac.cn; http://iopscience.iop.org/cpb

What follows is a list of articles you may be interested in

Optimization of glass-forming ability and synergistic enhancement of strength plasticity in $Cu_{50}Zr_{46}Al_4$ metallic glasses through Ag additions

Dongmei Li(李冬梅), Zhongyi Zhang(张忠一), Bolin Shang(尚博林), Rui Feng(丰睿), Xuefeng Li(李雪枫), and Peng Yu(余鹏)

Chin. Phys. B, 2025, 34 (**8**): 086107. DOI: 10.1088/1674-1056/adcea1

Atomic origin of minor alloying element effect on glass forming ability of metallic glass

Shan Zhang(张珊), Qingan Li(李庆安), Yong Yang(杨勇), and Pengfei Guan(管鹏飞)

Chin. Phys. B, 2025, 34 (**3**): 036105. DOI: 10.1088/1674-1056/ada756

Effect of Y element on atomic structure, glass forming ability, and magnetic properties of FeBC alloy

Jin-Hua Xiao(肖晋桦), Da-Wei Ding(丁大伟), Lin Li(李琳), Yi-Tao Sun(孙奕韬), Mao-Zhi Li(李茂枝), and Wei-Hua Wang(汪卫华)

Chin. Phys. B, 2024, 33 (**7**): 076101. DOI: 10.1088/1674-1056/ad3dd4

Structural origin for composition-dependent nearest atomic distance in Cu-Zr metallic glass

Chi Zhang(张驰), Hua-Shan Liu(刘华山), and Hai-Long Peng(彭海龙)

Chin. Phys. B, 2023, 32 (**11**): 116101. DOI: 10.1088/1674-1056/acce99

Spatial correlation of irreversible displacement in oscillatory-sheared metallic glasses

Shiheng Cui(崔世恒), Huashan Liu(刘华山), and Hailong Peng(彭海龙)

Chin. Phys. B, 2022, 31 (**8**): 086108. DOI: 10.1088/1674-1056/ac65f3

Yielding transition under oscillatory shear in metallic glasses

Nannan Ren(任楠楠)[1,†], Tiantian Meng(孟天天)[1], Hui Huang(黄慧)[1], Qunshuang Ma(马群双)[1,2,‡], Jun Fang(房军)[3], Qin Li(李勤)[3], and Weihuo Li(李维火)[1]

[1] *School of Materials Science and Engineering, Anhui University of Technology, Maanshan* 243032, *China*
[2] *Key Laboratory of Green Fabrication and Surface Technology of Advanced Metal Materials (Anhui University of Technology), Ministry of Education, Maanshan* 243002, *China*
[3] *Hohhot Colin Thermal Power Co., Ltd., Hohhot* 010030, *China*

(Received 15 October 2025; revised manuscript received 17 November 2025; accepted manuscript online 15 December 2025)

The yielding transition of amorphous solids remains a fundamental yet poorly understood issue in materials physics. In this work, we employ oscillatory shear to probe the yielding transition in metallic glasses (MGs) with various thermal histories. We identify three distinct deformation regimes depending on the applied strain amplitudes. Below the yield strain γ_y, the response is elastic and accompanied by aging, through reversible atomic rearrangements that preserve the material's initial memory of thermal history. Slightly above γ_y, the system undergoes a sharp transition during oscillatory cycles, indicated by a sudden rise in potential energy and non-affine displacement, along with the emergence of a shear band. Well above γ_y, plastic deformation dominates, driving samples of various initial stability toward a common steady state, while thermal histories are erased by irreversible rearrangements and shear band formation. These findings advance the understanding of failure mechanisms in MGs and shed light on tuning their mechanical performance in industrial applications involving cyclic loading.

Keywords: metallic glasses, mechanical property, oscillatory shear, molecular dynamics simulation

PACS: 61.43.Dq, 64.70.pe, 62.20.fg, 62.20.fq

DOI: 10.1088/1674-1056/ae2c6c **CSTR:** 32038.14.CPB.ae2c6c

1. Introduction

As the core of plastic flow and mechanical failure of amorphous solids, yielding represents a nonequilibrium transition between elastic and plastic states, which is a fundamental yet poorly understood phenomenon.[1–8] While the yielding behavior under traditional uniform shear has been extensively studied,[5–10] its irreversible and instantaneous nature poses significant challenges for directly capturing this dynamic process at the atomistic scale. In contrast, oscillatory shear offers a new perspective for studying the yielding phenomenon,[1–3,11–13] enabling precise probing of both macroscopic and microscopic behaviors on either side of the yield point through controlled oscillatory cyclic deformation.

Metallic glasses (MGs) are promising candidate materials for a wide range of structural and functional applications,[14] often subjected to cyclic deformation or repetitive loading.[15] Furthermore, oscillatory shear is extensively employed as an experimental technique to investigate the properties of MGs, with applications including fatigue tests,[16,17] dynamic mechanical analysis (DMA),[18] and, more recently, the use of ultrasonic vibrations to fabricate bulk MGs and enhance their plasticity.[19,20] Understanding the yielding transition of MGs under oscillatory shear is therefore critical not only for elucidating the failure mechanisms of MGs in complex practical scenarios, but also for uncovering the fundamental nature of yielding.[21,22]

Previous research on the oscillatory shear of amorphous solids has predominantly relied on the athermal quasistatic (AQS) approach, which has provided many valuable insights.[1,3,11,23–28] The strain amplitude γ_0 plays a critical role in determining the response to oscillatory shear:[1,3,11,27] small-amplitude strains can increase the stability of samples (i.e., overaging), whereas larger-amplitude strains typically increase energy, thereby "rejuvenating" the material. Numerous studies utilizing the AQS approach have revealed that yielding under oscillatory shear is fundamentally linked to irreversible rearrangements of particles.[26,28,29] In addition, the initial annealing degree also affects the mechanical behavior of model glasses under both uniform shear[8] and oscillatory shear.[1,25] However, the AQS approach neglects the effects of temperature and loading rate, while experimental oscillatory shear of MGs is typically conducted at finite temperatures and finite strain rates. Systematic studies on the yielding behavior of MGs under oscillatory shear at finite temperatures are still lacking, leaving the relative roles of strain amplitude and thermal annealing largely unclear.

In this work, the representative MG system $Cu_{64}Zr_{36}$ is selected for its good glass-forming ability and relatively high plasticity.[30,31] We aim to reveal the yielding transition under oscillatory shear in MGs from mechanical properties, poten-

†Corresponding author. E-mail: nnren@ahut.edu.cn
‡Corresponding author. E-mail: qunsma@ahut.edu.cn
© 2026 Chinese Physical Society and IOP Publishing Ltd. All rights, including for text and data mining, AI training, and similar technologies, are reserved.

tial energy, and atomic-scale dynamic features, and to clarify the distinctions between mechanical and thermal annealing.

2. Simulation details

Molecular dynamics (MD) simulations were performed using the LAMMPS package[32] on a typical MG system, $Cu_{64}Zr_{36}$, consisting of 50000 atoms. Periodic boundary conditions were applied in all three directions. The embedded atom method (EAM) potential[33] was used, and the time step was set to 2 fs. The $Cu_{64}Zr_{36}$ system was first equilibrated at 2000 K (well above the melting temperature) in the NPT ensemble using the Nosé–Hoover thermostat,[34] and then quenched to 300 K at a cooling rate of 1 K/ps, followed by relaxation for 1 ns at 300 K. To generate initial MG configurations with various stabilities, the as-prepared samples were annealed at initial temperatures (denoted as $T_{\rm init}$) of 2000 K, 1000 K, 900 K, 800 K, and 700 K. The annealed samples were then quenched to 300 K instantaneously by directly resetting the temperature and subsequently relaxed for 1 ns in the NVT ensemble. A sinusoidal shear strain $\gamma = \gamma_0 \sin(2\pi t/t_{\rm p})$ was applied to samples along the xy plane, with a period $t_{\rm p} = 50$ ps and strain amplitudes γ_0 ranging from 0.02 to 0.1. For each amplitude, three independent shear cycles were performed, starting from the same initial atomic configuration but with atomic velocities randomly assigned according to the Maxwell–Boltzmann distribution.

3. Results and discussion

We first investigate the behavior of macroscopic mechanical quantities under oscillatory shear. As shown in Fig. S1 of the supplementary materials, by fitting the time dependence of shear stress τ in steady state after enough cycles to $\tau = \tau_0 \sin(2\pi t/t_{\rm p} + \delta)$, where τ_0 is the stress amplitude and δ is the phase lag, a corresponding maximum stress τ_0 can be obtained for each maximum strain γ_0. Figure 1(a) shows the relation between τ_0 and γ_0 for all the samples. Under small γ_0, τ_0 increases as a result of oscillatory shear. When γ_0 exceeds a critical strain (~ 0.065), repeated shear leads to a sharp drop in τ_0, similar to the overshoot of the stress–strain curve in uniform shear, corresponding to yielding. Moreover, this overshoot is consistent with features of brittle yielding.[8] We identify this phenomenon as yielding under oscillatory shear, and the yield strain amplitude $\gamma_y \approx 0.065$. Above γ_y, τ_0 becomes largely independent of the strain amplitude and initial energy states, collapsing to a constant value across all samples.

Besides, we calculate the storage modulus as $G' = \tau_0 \cos(\delta)/\gamma_0$ and the loss modulus as $G'' = \tau_0 \sin(\delta)/\gamma_0$. The γ_0 dependence of these quantities is shown in Fig. 1(b) for different $T_{\rm init}$. At very low values of γ_0, G' maintains a high magnitude, while G'' is negligible (nearly zero). Both parameters exhibit only slight variations as γ_0 increases up to 0.065. This indicates a predominantly elastic response, consistent with the linear regime of the stress–strain curve in Fig. 1(a). Note that samples with lower $T_{\rm init}$ exhibit higher G' values, consistent with previous studies.[1] When γ_0 exceeds γ_y, G' undergoes an abrupt decrease, while G'' increases sharply, suggesting a notable reduction in elastic response and the onset of plastic deformation. The data of G' and G'' for γ_0 higher than γ_y almost collapse onto one main curve, irrespective of $T_{\rm init}$.

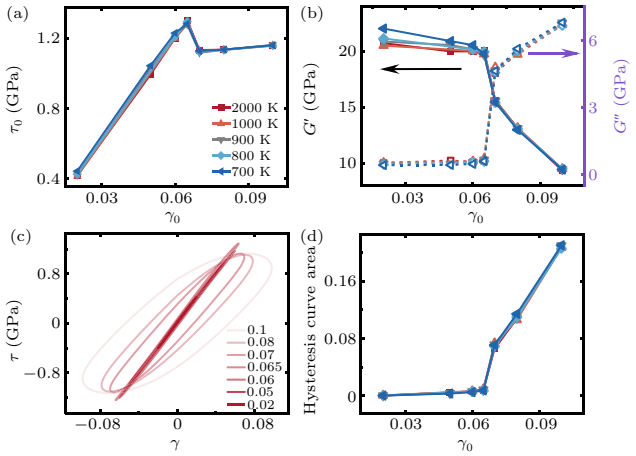


Fig. 1. Relations between maximum strain γ_0 and (a) maximum stress τ_0, and (b) storage modulus G' and loss modulus G'' in the steady state for all samples with different $T_{\rm init}$. (c) Stress–strain curves within one shear cycle under various γ_0 for the sample with $T_{\rm init} = 2000$ K. (d) Hysteresis loop area per cycle as a function of γ_0.

In Fig. 1(c), we display the averaged stress–strain curves over one cycle for the sample with $T_{\rm init} = 2000$ K as a representative. The shapes of the stress–strain hysteresis loops change noticeably with increasing γ_0. Under small γ_0, the stress–strain curves for loading and unloading processes nearly coincide, and the enclosed area of the hysteresis loop per cycle in the steady state is negligibly small, as shown in Fig. 1(d), indicating a predominantly elastic response with minimal energy dissipation. Beyond γ_y, the hysteresis loop becomes elliptical, approaching a parallelogram shape as γ_0 further increases. The area expands significantly, indicative of an increasing contribution of viscoelastic and plastic deformation associated with a substantial rise in energy dissipation. These results suggest that large-amplitude oscillatory shear effectively erases the "initial memory" of MG, whereas small-amplitude shear preserves it.

To analyze the roles of thermal and mechanical annealing, we study the potential energy evolution for various $T_{\rm init}$ and γ_0. In agreement with previous studies on model glasses,[25,35] Fig. 2(d) shows that the potential energy decreases with decreasing $T_{\rm init}$ in the absence of oscillatory shear ($\gamma_0 = 0$), directly demonstrating the enhanced stability of the initial states through thermal annealing. Under small γ_0 before yielding, oscillatory shear induces aging in all investigated samples, suggesting that cyclic shear at modest amplitudes drives poorly-

annealed MGs to deeper energy states, a phenomenon known as mechanical annealing.[35] As shown in Fig. 2(a), the decay of potential energy follows a stretched exponential function,[3] and the steady-state energy in Fig. 2(d) is obtained from the fitting. The inset of Fig. 2(a) shows that the potential energy during one cycle exhibits only a single, deep minimum near zero strain. Samples with higher $T_{\rm init}$ exhibit a greater reduction in potential energy after the same number of cycles, indicating that the extent of aging depends on $T_{\rm init}$ under small γ_0. By contrast, samples with lower $T_{\rm init}$, such as $T_{\rm init} = 700$ K, show negligible energy decrease and reach a steady state more readily. This indicates that thermal annealing at 700 K is sufficiently effective in stabilizing these MGs, so that mechanical annealing cannot further reduce their energy state. In other words, at small amplitudes, the MG samples largely retain their "initial memory". However, the differences among various $T_{\rm init}$ diminish with increasing γ_0 and ultimately vanish at the yield point, as shown in Fig. 2(d). Moreover, increasing γ_0 results in more extensive aging for a given sample, displaying a distinct crossover at the yield point. Our results demonstrate that mechanical annealing operates at small γ_0 ($< \gamma_y$) and high $T_{\rm init}$, but its efficiency diminishes as thermal annealing effects become dominant at lower $T_{\rm init}$.

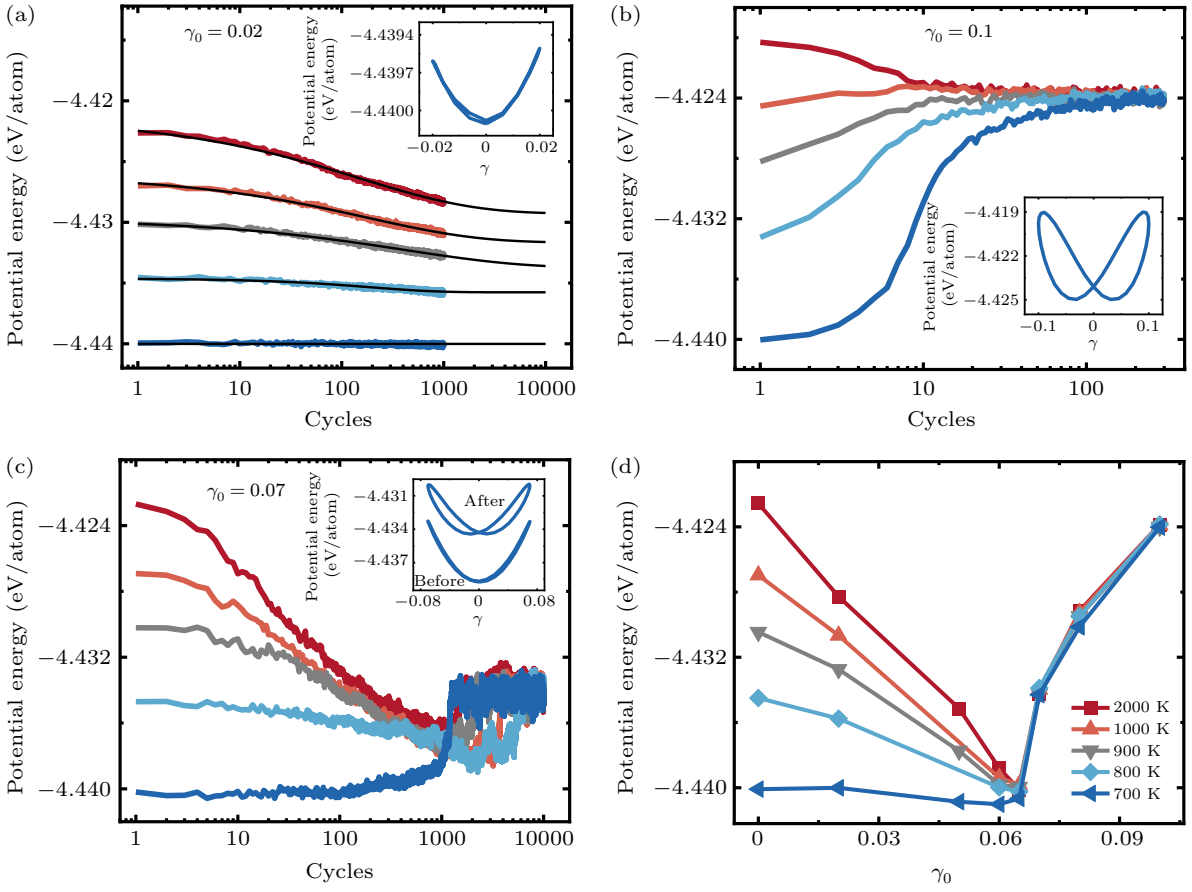


Fig. 2. Potential energy during oscillatory shear under maximum strains of 0.02 (a), 0.1 (b), and 0.07 (c) for all samples studied. The black lines in (a) are fits to a stretched exponential function, from which the steady-state energy values in (d) are obtained. The insets show the potential energy versus strain over one full shear cycle for the sample with $T_{\rm init} = 700$ K. Inset of (c): one full shear cycle before and after the abrupt transition under $\gamma_0 = 0.07$. (d) Relation between potential energy in the steady state and γ_0.

As observed in Fig. 2(b), under large amplitudes well above γ_y, samples with higher $T_{\rm init}$ exhibit aging, indicating that mechanical annealing is still effective, while those with lower $T_{\rm init}$ display rejuvenation. Despite these divergent pathways, all samples eventually reach the same steady state, independent of their initial energy conditions. The inset of Fig. 2(b) shows the double-minimum feature of potential energy in the steady state for large γ_0 above the yield point. Figure 2(d) shows that larger γ_0 leads to significantly higher steady-state energy. Furthermore, the number of cycles required to reach steady state is smaller for larger γ_0, as seen by comparing the results for $\gamma_0 = 0.1$ and 0.08 (see Fig. S3 of the supplementary materials). This suggests that larger amplitudes erase the "initial memory" of MGs more efficiently, driving the system toward a unique energy state regardless of $T_{\rm init}$. In this process, the initial energy conditions influence only the path toward the steady state (aging or rejuvenation), while the final energy depends solely on γ_0. It would be of interest to explore the response when reducing the strain amplitude after reaching the universal steady state at $\gamma_0 > \gamma_y$. As shown in Fig. S4

of the supplementary materials, after reaching the steady state under $\gamma_0 = 0.1$, all samples exhibit a similar trend of decreasing energy when the strain amplitude is suddenly reduced to 0.02, i.e., aging. The nearly identical energy evolution for all samples with different $T_{\rm init}$ also indicates that the initial memory of thermal history is effectively erased after achieving the steady state under large-amplitude oscillatory shear.

Different from the gradual evolution well above γ_y, the potential energy shows an abrupt rise after many cycles at $\gamma_0 = 0.07$, which is slightly above γ_y, as shown in Fig. 2(c). This behavior indicates the occurrence of a sudden yielding transition. Within a full cycle in the steady state, the potential energy exhibits a single minimum close to $\gamma_0 = 0$ before the transition, whereas after the transition it develops two distinct minima. The stress–strain curves in one cycle at $\gamma_0 = 0.07$ also show the corresponding emergence of loops (see Fig. S6 of the supplementary materials) with finite area, indicating the onset of viscoelasticity and plasticity.

To further examine atomic-scale local structural rearrangements under cyclic shear, we calculate the non-affine displacement ($D^2_{\rm min}$), which quantifies the deviation of atomic motions from a homogeneous affine deformation. The non-affine displacement of the i-th atom is defined as[36]

$$D^2_{{\rm min}\,i}(t,\Delta t) = \frac{1}{N_i}\sum_{k\in N_i}\{\boldsymbol{r}_{ik}(t+\Delta t) - \boldsymbol{J}_i\cdot\boldsymbol{r}_{ik}(t)\}^2,$$

where N_i is the number of neighboring atoms of atom i, $\boldsymbol{r}_{ik}(t) = \boldsymbol{r}_k(t) - \boldsymbol{r}_i(t)$ is the position vector of atom k relative to atom i at time t, and $\boldsymbol{J}_i$ is the local deformation gradient tensor. Here, Δt is chosen as $t_{\rm p} = 50$ ps, i.e., $D^2_{\rm min}$ is calculated using configurations separated by one period.

Figure 3(a) shows the average $D^2_{\rm min}$ during cyclic shear under small γ_0 ($= 0.02$). Following an initial increase over the first several cycles due to activation of local rearrangements, $D^2_{\rm min}$ subsequently decreases and approaches relatively small values after sufficient cycles. Figure 3(d) shows the dependence of steady-state $D^2_{\rm min}$ on γ_0 for various $T_{\rm init}$, remaining very small without significant changes below γ_y. These results suggest that under small-amplitude cyclic shear, atomic motion in the steady state is highly localized and largely reversible, allowing the sample to retain a structure close to its initial configuration.

At large amplitudes above γ_y, taking $\gamma_0 = 0.1$ in Fig. 3(b) as an example, $D^2_{\rm min}$ first increases and then saturates at a nearly constant value, much higher than that for $\gamma_0 = 0.02$. Large-amplitude shear induces irreversible atomic rearrangements and even collective flow, driving all samples toward a common steady state independent of initial energy conditions. Samples with higher $T_{\rm init}$ reach the plateau faster, indicating that looser and more disordered atomic structures are more readily driven to the steady state. Figure 3(c) shows $D^2_{\rm min}$ for $\gamma_0 = 0.07$, slightly above γ_y, which also exhibits a sharp increase and reaches the same plateau, similar to the potential energy results. Furthermore, Fig. 3(d) shows that the dependence of steady-state $D^2_{\rm min}$ on γ_0 displays a distinct crossover at γ_y, indicating that the yielding transition corresponds to an abrupt increase of non-affine displacements in the system.

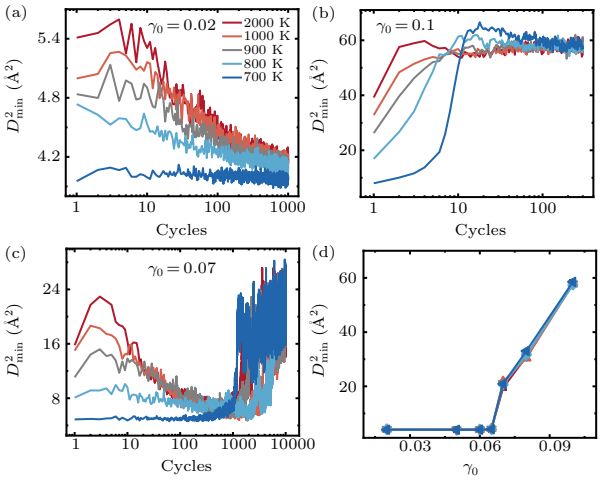


Fig. 3. Average non-affine displacement $D^2_{\rm min}$ during oscillatory shear under $\gamma_0 = 0.02$ (a), 0.1 (b), and 0.07 (c) for all samples. (d) Average $D^2_{\rm min}$ in the steady state as a function of γ_0.

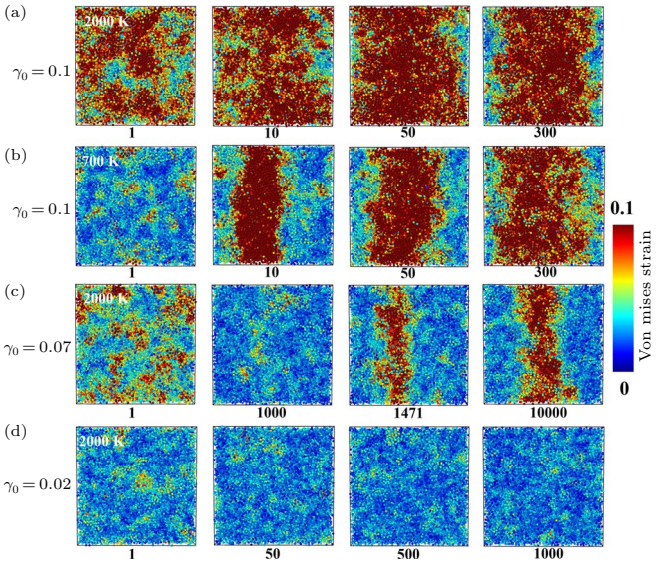


Fig. 4. Spatial distributions of Von Mises strain under cyclic shear. Samples with $T_{\rm init} = 2000$ K (a) and 700 K (b) under $\gamma_0 = 0.1$. Samples under $\gamma_0 = 0.07$ (c) and 0.02 (d) for $T_{\rm init} = 2000$ K. The corresponding shear cycle numbers are indicated below each snapshot.

In order to visualize atomic rearrangements in MGs during cyclic shear with different $T_{\rm init}$ and γ_0, Fig. 4 presents the spatial distribution of the von Mises strain.[37] Figures 4(a) and 4(b) illustrate the initiation and propagation of shear bands under amplitudes well above γ_y. As shown in Fig. 4(a), a shear band develops gradually after many cycles in samples starting from a high-energy state ($T_{\rm init} = 2000$ K). In contrast, a thin, localized shear band, referred to as an initial shear band, forms rapidly within just a few cycles in samples with lower $T_{\rm init}$ (see

Fig. 4(b) for $T_{\text{init}} = 700$ K), which eventually broadens into a wider shear band. These observations are consistent with findings reported by Ozawa *et al.*[8] for well-annealed glasses under uniform shear, where initial shear bands were shown to originate from structural memory. Despite these different pathways, shear bands in both high-T_{init} and low-T_{init} samples eventually exhibit comparable morphologies under $\gamma_0 = 0.1$, indicating that large shear amplitudes effectively erase the initial structural memory. In addition, samples with higher T_{init} are more readily activated during the first shear cycle, generating more shear transformation zones (STZs). Note that shear bands gradually disappear when reducing the strain amplitude after reaching the universal steady state (see Fig. S7 of the supplementary materials), accompanying the aging regime, which has been referred to as shear band healing in previous studies.[2]

As shown in Fig. 4(c), two regimes are observed during long-time shear cycles at $\gamma_0 = 0.07$: (i) continuously small von Mises strain corresponding to structural relaxation and enhanced stability; (ii) a subsequent abrupt formation of a thin shear band within several cycles. All samples ultimately develop similar shear band morphologies, corresponding to identical energy states (see Fig. S8 of the supplementary materials). For comparison, Fig. 4(d) shows the spatial distribution under low amplitude, far below γ_y, where no shear bands are observed during cyclic shear. Moreover, the decreasing number of STZs with ongoing oscillatory shear indicates increasing structural stability of MG samples. These results demonstrate that shear band formation, involving large-scale atomic rearrangements, is key to erasing the memory of the initial state at $\gamma_0 > \gamma_y$.

The present study was performed at a fixed frequency. Based on previous studies showing that increasing the strain rate tends to delay yielding by limiting atomic rearrangements,[4,38] we expect the yield strain γ_y to increase with frequency. A systematic investigation of frequency effects will be an important direction for future work. Furthermore, an intriguing implication of mechanical aging observed at small strain amplitudes ($\gamma_0 < \gamma_y$) is its potential as a tool to produce ultra-stable glasses.[39,40] As shown in Fig. S10 of the supplementary materials, mechanical aging effectively drives poorly-annealed samples ($T_{\text{init}} = 2000$ K) to energy states lower than those of well-annealed samples ($T_{\text{init}} = 700$ K). This suggests that by appropriately tuning strain amplitude, temperature, and number of cycles, it may be possible to drive a rapidly quenched glass sample into an energy state comparable to or even lower than that achievable via conventional thermal annealing, offering a novel pathway for stabilizing amorphous materials.

4. Conclusion

In conclusion, this work systematically investigates the yielding transition of metallic glasses (MGs) under oscillatory shear, starting from different initial energy conditions. When the applied strain amplitude is below the yield point γ_y, the mechanical response is primarily elastic, and aging occurs across all samples. Atomic motions are confined to small, reversible rearrangements without shear band formation, thereby preserving the initial memory due to thermal annealing. Near the critical strain amplitude γ_y, both potential energy and nonaffine displacement (D^2_{min}) exhibit an abrupt increase after sufficient cycles, associated with the sudden emergence of a localized shear band. At amplitudes well above γ_y, plastic deformation becomes dominant. Both aging and rejuvenation drive various samples toward a common steady state, independent of their initial energy conditions. This regime is characterized by irreversible atomic-scale rearrangements and the formation of shear bands with similar morphologies in the steady state, demonstrating that large-amplitude oscillatory shear effectively erases the initial memory of thermal history. These findings provide deeper insight into the yielding mechanism of MGs and suggest strategies for tuning their mechanical properties in industrial applications involving cyclic deformation.

Acknowledgments

This project was supported by the National Natural Science Foundation of China (Grant Nos. 52201169 and 52575352) and the Key Research & Development Plan of Anhui Province (Grant No. 2022a05020016).

References

[1] Yeh W T, Ozawa M, Miyazaki K, Kawasaki T and Berthier L 2020 *Phys. Rev. Lett.* **124** 225502
[2] Parmar A D S, Kumar S and Sastry S 2019 *Phys. Rev. X* **9** 021018
[3] Leishangthem P, Parmar A D S and Sastry S 2017 *Nat. Commun.* **8** 14653
[4] Bonn D, Denn M M, Berthier L, Divoux T and Manneville S 2017 *Rev. Mod. Phys.* **89** 35005
[5] Pan J, Ivanov Y P, Zhou W H, Li Y and Greer A L 2020 *Nature* **578** 559
[6] Schuh C A and Lund A C 2003 *Nat. Mater.* **2** 449
[7] Cheng Y Q and Ma E 2011 *Acta Mater.* **59** 1800
[8] Ozawa M, Berthier L, Biroli G, Rosso A and Tarjus G 2018 *Proc. Natl. Acad. Sci. USA* **115** 6656
[9] Zhang Z, Ding J and Ma E 2022 *Proc. Natl. Acad. Sci. USA* **119** e2213941119
[10] Shang B 2023 *Chin. Phys. B* **33** 16102
[11] Cochran J O, Callaghan G L, Caven M and Fielding S M 2024 *Phys. Rev. Lett.* **132** 168202
[12] Singh M, Ozawa M and Berthier L 2020 *Phys. Rev. Mater.* **4** 025603
[13] Priezjev N V 2021 *Comp. Mater. Sci.* **200** 110831
[14] Wang W H 2019 *Prog. Mater. Sci.* **106** 100561
[15] Tang X, Deng J, Mo Y, Meng L and Yao X 2023 *Sci. Sin. Phys.* **54** 254602 (in Chinese)
[16] Priezjev N V 2023 *Metals* **13** 1606
[17] Liang S Y, Zhang L T, Wang Y J, Wang B, Pelletier J M and Qiao J C 2024 *Int. J. Fatigue* **187** 108446

[18] Wang B, Wang L J, Shang B S, Gao X Q, Yang Y, Bai H Y, Pan M X, Wang W H and Guan P F 2020 *Acta Mater.* **195** 611
[19] Sohrabi S, Fu J, Li L, Zhang Y, Li X, Sun F, Ma J and Wang W H 2024 *Prog. Mater. Sci.* **144** 101283
[20] Ma J, Yang C, Liu X, Shang B, He Q, Li F, Wang T, Wei D, Liang X, Wu X, Wang Y, Gong F, Guan P, Wang W and Yang Y 2019 *Sci. Adv.* **5** x7256
[21] Kamani K M and Rogers S A 2024 *Proc. Natl. Acad. Sci. USA* **121** e1893558175
[22] Radhakrishnan R and Fielding S M 2016 *Phys. Rev. Lett.* **117** 188001
[23] Shang B, Wang W and Guan P 2022 *Acta Mater.* **225** 117557
[24] Khirallah K, Tyukodi B, Vandembroucq D and Maloney C E 2021 *Phys. Rev. Lett.* **126** 218005
[25] Bhaumik H, Foffi G and Sastry S 2021 *Proc. Natl. Acad. Sci. USA* **118** e2100227118
[26] Das P, Vinutha H A and Sastrya S 2020 *Proc. Natl. Acad. Sci. USA* **117** 10203
[27] Fiocco D, Foffi G and Sastry S 2013 *Phys. Rev. E* **88** 20301
[28] Cui S, Liu H and Peng H 2022 *Chin. Phys. B* **31** 86108
[29] Khushika A, Laurson L and Jana P K 2023 *Phys. Rev. E* **108** 64612
[30] Liu Y, Yang Z, Yang Y, Luo J and Huang X 2024 *J. Non-Cryst. Solids* **629** 122891
[31] Li Y, Guo Q, Kalb J A and Thompson C V 2008 *Science* **322** 1816
[32] Plimpton S 1995 *J. Comput. Phys.* **117** 1
[33] Mendelev M I, Kramer M J, Ott R T, Sordelet D J, Yagodin D and Popel P 2009 *Philos. Mag.* **89** 967
[34] Hoover W G 1985 *Phys. Rev. A* **31** 1695
[35] Priezjev N V 2018 *J. Non-Cryst. Solids* **479** 42
[36] Falk M L and Langer J S 1998 *Phys. Rev. E* **57** 7192
[37] Fan Y, Iwashita T and Egami T 2014 *Nat. Commun.* **5** 5083
[38] Cao T, Zhang Q, Wang L 2023 *Acta Mater.* **260** 119343
[39] Zhao Y, Shang B, Zhang B 2022 *Sci. Adv.* **8** n3623
[40] Zhao Y, Zhao Y and Wang D 2022 *Phys. Rev. X* **12** 031021